Published in Optics Express 13, issue 18, 7017-7027, 2005
which should be used for any reference to this work

A virtual optical probe based on localized Surface Plasmon Polaritons

Emiliano Descrovi, Vincent Paeder, Luciana Vaccaro and Hans-Peter Herzig

Institute of Microtechnology, University of Neuchâtel,
rue A.-L. Breguet 2, Neuchâtel 2000, Switzerland
emiliano.descrovi@unine.ch

Abstract: A confined, evanescent nano-source based on the excitation of Surface Plasmon Polaritons (SPP) on structured thin metal films is proposed. With the help of a suitable cavity, we numerically demonstrate that it is possible to trap SPP over a spatial region smaller than the diffraction limit. In particular, the enhanced plasmonic field associated with the zero-order cavity mode can be used as a virtual probe in scanning near-field microscopy systems. The proposed device shows both the advantages of a localized, non-radiating source and the high sensitivity of SPP-based sensors. The lateral resolution is limited by the lateral extension of the virtual probe. Results from simulated scans of small objects reveal that details with feature sizes down to 50 nm can be detected.

References and links

1. L. Novotny, E. J. Sánchez and X. S. Xie, "Near-field imaging using metal tips illuminated by higher-order Hermite-Gaussian beams," Ultramicroscopy **71,** 21–29 (1998).
2. E. Betzig and J. K. Trautman, T. D. Harris, J. S. Weiner and R. L. Kostelak, "Breaking the diffraction barrier: optical microscopy on a nanometric scale," Science **251,** 1468–1470 (1991).
3. L. Aeschimann, T. Akiyama, U. Staufer, N. F. de Roij, L. Thiery, R. Eckert and H. Heinzelmann, "Characterization and fabrication of fully metal-coated scanning near-field optical microscopy SiO_2 tips," J. Microsc. **209,** 182–187 (2003).
4. L. Vaccaro, L. Aeschimann, U. Staufer and H. P. Herzig, "Propagation of the electromagnetic field in fully coated near-field optical probes," Appl. Phys. Lett. **83,** 584–586 (2003).
5. A. Bouhelier, M. R. Beversluis and L. Novotny, "Near-field scattering of longitudinal fields," Appl. Phys. Lett. **82,** 4596–4598 (2003).
6. E. Descrovi, L. Vaccaro, W. Nakagawa, L. Aeschimann, U. Staufer and H. P. Herzig, "Collection of transverse and longitudinal fields by means of apertureless nanoprobes with different metal coating characteristics," Appl. Phys. Lett. **85,** 5340–5342 (2004).
7. E. Descrovi, L. Vaccaro, L. Aeschimann, W. Nakagawa, U. Staufer and H. P. Herzig, "Optical properties of microfabricated fully metal-coated near-field probes in collection mode," J. Opt. Soc. Am. A , *in press*
8. T. Grosjean and D. Courjon, "Immaterial tip concept by light confinement," J. Microsc. **202,** 273–278 (2000).
9. T. Grosjean, D. Courjon and D. Van Labeke, "Bessel beams as virtual tips for near-field optics," J. Microsc. **210,** 319–323 (2003).
10. Tao Hong, Jia Wang, Liqun Sun and Dacheng Li, "Numerical simulation analysis of a near-field optical virtual probe," Appl. Phys. Lett. **81,** 3452–3454 (2002).
11. W. L. Barnes, A. Dereux and T. W. Ebbesen, "Surface plasmon subwavelength optics," Nature (London) **424,** 824–830 (2003).
12. W. L. Barnes, S. C. Kitson, T. W. Preist and J. R. Sambles, "Photonic surfaces for surface-plasmon polaritons," J. Opt. Soc. Am. A **14,** 1654–1661 (1997).
13. S. C. Kitson, W. L. Barnes and J. R. Sambles, "Full Photonic Band Gap for Surface Modes in the Visible," Phys. Rev. Lett. **77,** 1670–2673 (1996).

14. S. I. Bozhevolnyi, J. Erland, K. Leosson, P. M. W. Skovgaard and J. M. Hvam, "Waveguiding in Surface Plasmon Polariton Band Gap Structures," Phys. Rev. Lett. **86,** 3008–3011 (2001).
15. T. Okamoto, F. HDhili and S. Kawata, "Towards plasmonic band gap laser," Appl. Phys. Lett. **85,** 3978–3970 (2004).
16. A. Bouhelier, T. Huser, H. Tamaru, H. J. Güntherodt, D. W. Pohl, Fadi I. Baida and D. Van Labeke, "Plasmon optics of structured silver films," Phys. Rev. B **63,** 155404-1–155404-9 (2001).
17. H. Ditlabacher, J. R. Krenn, G. Schider, A. Leitner and F. R. Aussenegg, "Two-dimensional optics with surface plasmon polaritons," Appl. Phys. Lett. **81,** 1762–1764 (2002).
18. D. C. Skigin and R. A. Depine, "Surface shape resonances and surface plasmon polariton excitations in bottle-shaped metallic gratings," Phys. Rev. E **63,** 046608-1–046608-10 (2001).
19. S. C. Kitson, W. L. Barnes and J. R. Sambles, "Photonic band gaps in metallic microcavities," J. Appl. Phys. **84,** 2399–2403 (1998).
20. K. M. Engenhardt and S. Gregory, "Surface-plasmon-polariton excitation of optical microcavities and second-harmonic emission," J. Opt. Soc. Am. B **17,** 593–599 (2000).
21. P. André, F. Charra and M. P. Pileni, "Resonant electromagnetic field cavity between scanning tunneling microscope tips and substrate," J. Appl. Phys. **91,** 3028–3036 (2002).
22. T. Okamoto, T. Kobayashi and I. Yamaguchi, "Local plasmon sensor with gold colloid monolayers deposited upon glass subtrates," Opt. Lett. **25**, 372–374 (2000).
23. C. Rockstuhl, M. Salt and H. P. Herzig, "Analyzing the scattering properties of coupled metallic nano-particles," J. Opt. Soc. Am. A, **21**, 1761–1768 (2004)
24. L. Li, J. Chandezon, G. Granet and J. P. Plumey, "Rigorous and efficient grating-analysis method made easy for optical engineers," Appl. Opt. **38,** 304–313 (1999).
25. L. Li, G. Granet, J. P. Plumey and J. Chandezon, "Some topics in extending the C method to multilayer gratings of different profiles," Pure Appl. Opt. **5,** 141–156 (1996).
26. W. L. Barnes, T. W. Preist, S. C. Kitson, J. R. Sambles, "Physical origin of photonic energy gaps in the propagation of surface plasmons on gratings," Phys. Rev. B **54,** 6227–6244 (1996).
27. W. L. Barnes, T. W. Preist, S. C. Kitson, J. R. Sambles, N. P. K. Cotter and D. J. Nash, "Photonic gaps in the dispersion of surface plasmons on gratings," Phys. Rev. B **51,** 11164–11167 (1995).
28. W.-C. Tan, T. W. Preist, J. R. Sambles, M. B. Sobnack and N. P. Wanstall, "Calculation of photonic band structures of periodic multilayer grating systems by use of a curvilinear coordinate transformation", J. Opt. Soc. Am. A **15**, 2365–2372 (1998).
29. P. B. Johnson and R. W. Christy, "Optical constants of the noble metals," Phys. Rev. B **6,** 4370–4379 (1972).
30. J. R. Krenn, H. Ditlbacher, G. Schider, A. Hoheanau, A. Leitner and F. R. Aussenegg, "Surface plasmon micro and nano-optics," J. Microsc. **209,** 167–172 (2002).
31. B. Fisher, T. M. Fisher and W. Knoll, "Dispersion of surface plasmons in rectangular, sinusoidal and inchoerent silver gratings," J. Appl. Phys. **75,** 1577–1581 (1994).
32. E. Silberstein, P. Lalanne, J. P. Hugonin and Q. Cao, "Use of gratings theories in integrated optics," J. Opt. Soc. Am. A **18**, 2865–2875 (2001)
33. D. Peyrade, E. Silberstein, P. Lalanne, A. Talneau and Y. Chen, "Short Bragg mirrors with adiabatic modal conversion," Appl. Phys. Lett. **81,** 829–831 (2002).

1. Introduction

One of the basic requirements of many super-resolving imaging systems is to illuminate the sample with a highly confined optical field. Well-established Scanning Near-field Optical Microscopy (SNOM) techniques can accomplish this in different ways. For example, it is possible to obtain a localized field by tightly focusing higher-order Hermite-Gaussian beams on metal tips, which can be employed as nano-sources [1]. Another possibility is to use metal-coated tapered monomode optical fibers having a subwavelength hole at the apex [2] or microfabricated fully metal-coated probes [3]. Some investigations based on numerical calculations (see, for example, Ref. [4]) and experimental measurements [5, 6, 7] revealed that the strongest localization of the emitted field is connected to the presence of a longitudinally polarized field. Nonetheless, the main drawback in the exploitation of such a field is the necessity of the probe itself, which is, in general, fragile and difficult to reproduce on a large scale.

One solution to this problem was suggested by Grosjean *et al.* [8, 9], who proposed the use of virtual (or immaterial) tips, in near-field microscopy. In those papers, the authors describe the concept of a virtual tip as a purely evanescent pattern obtained by suitable interference of radially polarized Bessel-Gauss beams at the hemispherical surface of an axicon element. The

experimental setup allowed the generation of an evanescent, non-diffracting and longitudinally polarized field confined over a circular region of diameter $\sim \lambda/5$, to be used for sample illumination. Another realization of a non-radiating source is presented in Ref. [10], where the combined use of interfering waves and filtering masks produced a virtual optical probe having FWHM $= 0.42\lambda$.

In this paper, we consider an innovative solution for a non-radiating and highly spatially confined light source. Such a source is obtained by a proper excitation of Surface Plasmon Polaritons (SPP). In particular, the field enhancement produced by SPP excited in a suitable Distributed Feedback System (DFS) can be used as a virtual optical probe. During the few last years, optical phenomena linked to SPP have attracted attracted gaining interest, mainly due to the possibilities of applications such as plasmonic crystals and photonic surfaces [11, 12, 13, 14], plasmonic band gap lasers [15] and two-dimensional optics [16, 17]. A number of different types of metallic micro-cavities for SPP have also been considered in the past: most of them being buried in the metal film [18] or placed out-of-plane with respect to the propagation direction of SPP [19, 20, 21]. In the present work we consider the possibility of using a plasmonic field as a nano-source for near-field microscopy. This choice is particularly interesting for several reasons. Most importantly, as will be shown, the proposed device couples the benefits of highly-sensitive, plasmon-based sensors [22] and strongly confined, non-radiating sources.

SPP can be coupled on metallic nano-particles or metallic surfaces. A strong field localization effect can be observed with metallic nano-particles [23], but it is hard to exploit it because of the practical difficulty of handling small objects. Alternatively, SPP localization can be achieved by structuring planar metallic surfaces. We propose a flat surface surrounded by a pair of sinusoidal gratings acting as Distributed Bragg Reflectors (DBR) for surface waves. With this configuration, as SPP are trapped in the flat region by the DBRs, they show a cavity-like resonating behavior. The field enhancement associated with the lowest order mode is then used as a plasmonic virtual probe.

In order to perform our numerical analysis, we implemented the differential method of Chandezon, the C-method, (see, for example, Ref. [24]) and its extension to multilayered periodic gratings proposed in Ref. [25]. This method is particularly suited for studying this kind of problem since it allows smooth grating profiles to be considered without performing any multi-layer structure discretization [12, 26, 27, 28].

2. Excitation of surface plasmon polaritons on flat and corrugated surfaces

Surface Plasmon Polaritons are associated with strong electromagnetic fields confined at metal-dielectric interfaces, where the real part of the permittivities of the two media have opposite signs. SPP can be excited under specific illumination conditions: in the following we will consider the two-dimensional Kretschmann configuration, as shown in Fig. 1.

A thin film of silver is deposited on the flat surface of a semi-cylindrical glass lens. The incident radiation is a p-polarized plane wave passing through the glass and then impinging on the metal layer with a varying angle θ with respect to the surface normal. The illuminating plane wave is associated with a magnetic field vector having amplitude $|H_0| = 1$ and orientation parallel to the z-axis. The coupling of photons to plasmon polaritons at the metal-air interface is monitored by means of the normalized coefficients R and T, defined as the sum of the reflected and transmitted order efficiencies (η_i^r and η_i^t, with $i = 0, \pm 1, \pm 2, \ldots$) as shown in Eq. (1):

$$R = \sum_i \eta_i^r \quad , \qquad T = \sum_i \eta_i^t . \tag{1}$$

The values of the permittivities of Silver $\varepsilon_{Ag}(\lambda)$ used in the calculations are taken from Johnson and Christy [29].

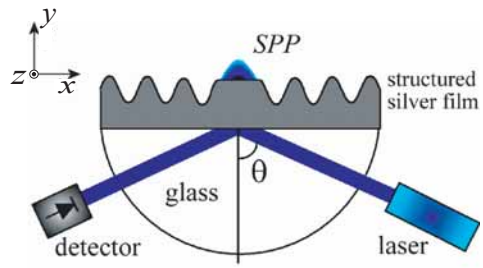

Fig. 1. Excitation of Surface Plasmon Polaritons in the Kretschmann-Raether configuration. Light incident at angle θ with respect to the surface normal, hits the silver film deposited on the flat surface of a cylindrical glass lens and is then reflected. The reflected light is used to monitor the coupling of photons with plasmon polaritons at the metal interface.

In order to realize a DBR, we first determine the conditions under which SPP can be coupled on a flat silver film surface and subsequently calculate the SPP wave vector associated with the propagation along the silver-air interface. The spatial periodicity of SPP is determined by the real part $Re\{k_{\|}\}$ of the wave vector component parallel to the interface. Once $Re\{k_{\|}\}$ is calculated, a suitable corrugation of the silver film is introduced in order to make a one-dimensional DBR for SPP [30].

First we consider a flat silver film of thickness $t = 50$ nm. The parameter R is calculated for different illumination wavelengths λ and different incidence angles θ, according to the setup of Fig. 1. The map of the reflection coefficient $R(\lambda,\theta)$ is shown in Fig. 2 (linear color scale).

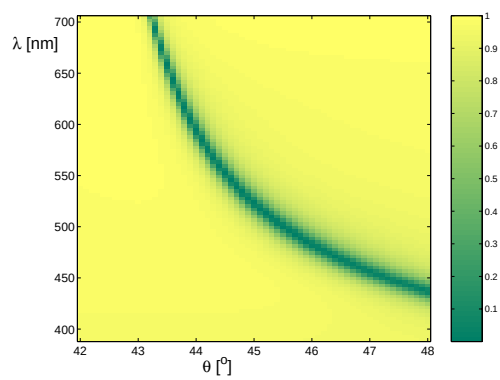

Fig. 2. Calculated map of the reflection coefficient $R(\lambda,\theta)$ of a flat thin silver film ($t = 50$ nm) illuminated in the Kretschmann-Raether configuration at different wavelengths λ and incidence angles θ. Dark zones (low reflectivity) correspond to the excitation of SPP.

The dark region corresponds to diminished reflected light intensity, where an efficient transfer of radiative energy to SPP modes occurs. If we restrict our attention to $\lambda = 470$ nm and $\theta = 45.4^{\circ}$ we can excite a SPP having wave vector $Re\{k_{\|}\} = 14.248\ \mu\text{m}^{-1}$. Since the simplest Bragg mirror couples the incident and the reflected light via its first harmonic component, we structure the metal-air interface of the silver film with a purely sinusoidal profile having period $\Lambda \approx \pi / Re\{k_{\|}\}$. Consequently, a frequency band gap in the SPP excitation curve is expected to open [31, 26]. We consider the case of a sinusoidal corrugation having a period of $\Lambda = 220$ nm

and an amplitude of $h = 10$ nm. The result is reported in Fig. 3. The SPP-coupling region of Fig. 2 is split into two arms by the presence of the periodic modulation of the surface. The center of the band gap can be tuned to different wavelengths along the SPP excitation curve, depending on the period of the modulation Λ and on the illumination angle θ. The two standing SPP waves excited at the edges of the gap present the same spatial periodicity while having different energies as shown in Ref. [27].

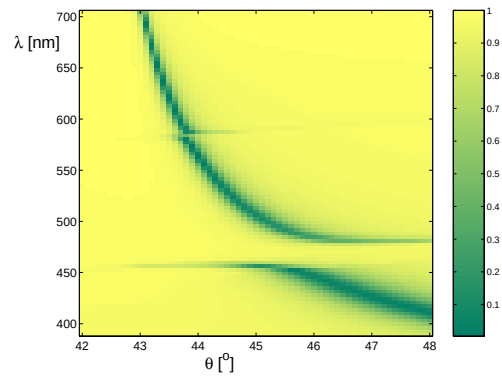

Fig. 3. Calculated map of the reflection coefficient $R(\lambda, \theta)$ of a thin silver film illuminated in the Kretschmann-Raether configuration at different wavelengths λ and incidence angles θ. The metal-air interface is corrugated with a sinusoidal profile of period $\Lambda = 220$ nm. A band gap at $\lambda \approx 470$ nm emerges due to the presence of the corrugation.

3. Microcavities for surface plasmon polaritons

The cavity we propose consists of a flat surface region surrounded by DBR on both sides. Two possible arrangements are considered, as shown in Fig. 4. In the case of Fig. 4(a) the modulation is a raised profile on the surface of the metal layer, while in the case of Fig. 4(b) the modulation is etched into the metal layer. In both cases, the silver film thickness corresponding to the flat region is $t = 50$ nm.

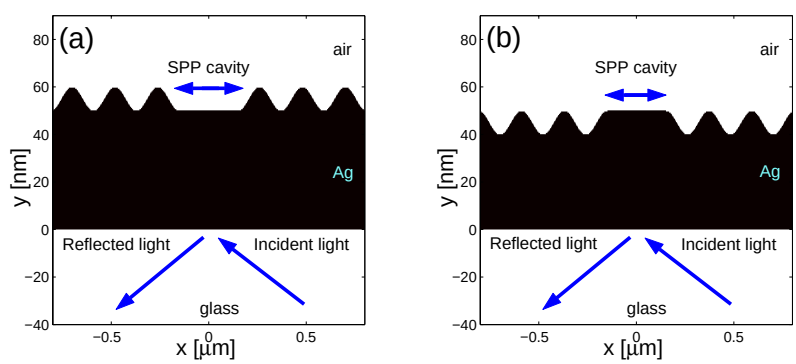

Fig. 4. Topographic profiles of two possible configurations of the cavity. In case (a) the modulation is a raised profile on the surface of the metal layer, while in case (b) it is etched into the layer.

The C-method is a Fourier-based method for solving periodic diffraction problems. Therefore, the case of a single cavity surrounded by Bragg mirrors cannot be treated directly with such a

method, since an infinite calculation domain should be considered. Nevertheless, approximate solutions are possible, for example by using a super-lattice of cavities. Each cavity is separated from its neighbors by a Distributed Bragg Reflector (DBR) of finite length. In such a situation, a critical parameter is the length of the DBR: too large DBRs are impractical, while too short DBRs allow strong cross-talk effects between cavities. Spurious cross-talks can be reduced using several approaches (see, for example, Ref. [32]). In our case, we performed a preliminary set of test calculations in order to find a reasonable value for the DBR length. We monitored the field enhancement factor associated with the SPP inside the cavity as a function of the number of DBR periods on each side of the flat region. The result is shown in Fig. 5.

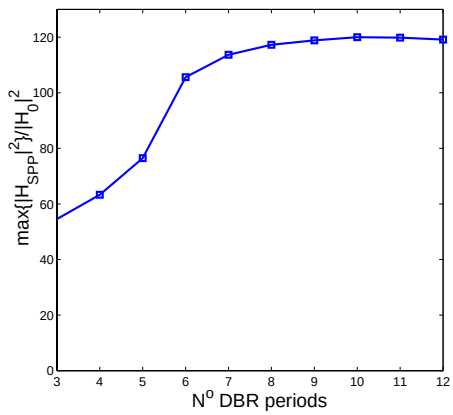

Fig. 5. Convergence of the field enhancement factor as a function of the number of DBR periods at each side of the flat region considered in the calculations.

The influence of the cross-talk has been evaluated by calculating the field enhancement inside the cavity as $max\left\{|H_{SPP}(x,y)|^2\right\}/|H_0|^2$. We observed that the field enhancement factor converges asymptotically as the length od the DBR increases. If the number of DBR periods is ≥ 8, the field enhancement factor shows small variations $\leq 1\%$. The compromise we adopted is to consider 10 grating periods on each side of the cavity.

In Fig. 6 the coefficients R and T are plotted as functions of the cavity length L. Data points associated with the minima of R and maxima of T correspond to the excitation of different modes in the cavity. The zero- and the first- order modes are found at $L_{n=0} = 112$ nm and $L_{n=1} = 330$ nm respectively. Calculations are in good agreement with the prediction of the well-known formula

$$Re\{k_{\|}\} \cdot L \sim (2n+1)\pi/2 \tag{2}$$

This result demonstrates the resonant behavior of the structure under investigation. Both configurations shown in Fig. 4 present the same behavior. The ripple effect present in the T profile is mostly liked due to a secondary resonance which has no significative impact on the performances of the device. It is interesting to remark that, close to the resonance points, the SPP is partially converted into free-space propagating photons, as the non-zero value of the transmission coefficient demonstrates. This phenomenon is attributed to the scattering performed by the surface discontinuities at the cavity boundaries. A similar effect is also frequently observed in the case of photonic crystals. In order to minimize this effect it has been demonstrated that it is possible to design modulated profiles to achieve adiabatic mode conversion between the topographically different regions of space [33]. Unfortunately, in our case, a smoother change between allowed (flat region) and forbidden (DBR) regions would present a drawback in terms

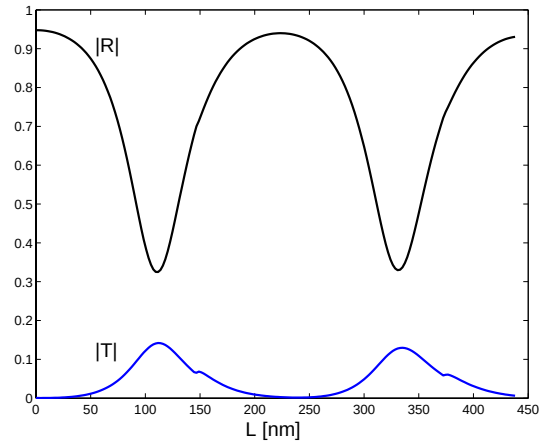

Fig. 6. Reflection (R) and transmission (T) coefficients of a DFS for SPP for different lengths of the flat region. The two plots show a typical resonance profile.

of quality of the virtual tip as will be shown in the next section.

4. Plasmonic virtual probe

The goal of this work is to demonstrate that a localized, non-radiating light nano-source can be realized by coupling SPP onto a suitable resonant metallic structure. For this reason, we focused our attention on the lowest-order cavity mode. Calculations of the squared amplitude distribution of the magnetic field associated with the zero-order are shown in Fig. 7 for both of the considered configurations. At the metal-air interface, a field enhancement factor $max\left\{|H_{SPP}(x,y)|^2\right\}/|H_0|^2 = 120$ is found.

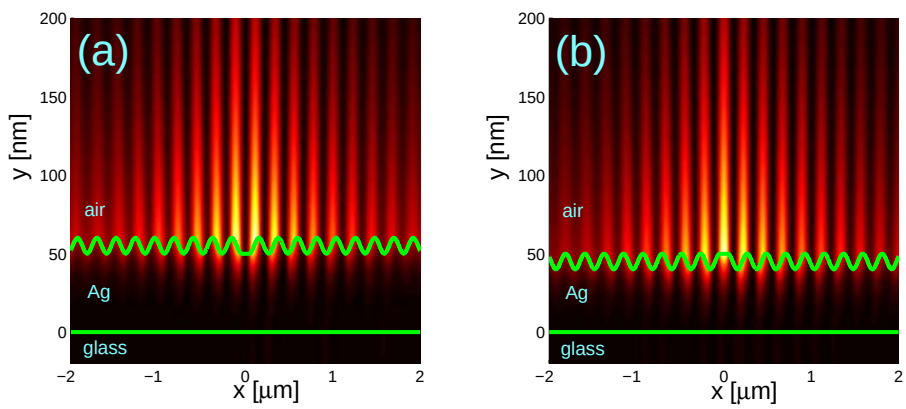

Fig. 7. Squared amplitude of the magnetic field associated with the plasmonic zero-order mode excited in the two considered DFS configurations: (a) raised profile, (b) etched profile.

Although the lowest order modes are excited in both cases at the same cavity length $L_{n=0} = 112$ nm, their near-field distributions are significantly different. In fact, in the case (a), the $n = 0$ mode has a node in the center of the flat region, while in case (b) it shows a maximum of amplitude. The presence of the two lobes makes the configuration (a) unusable to generate a

single, localized and non-radiating light source. On the other hand, configuration (b) is more interesting for our purposes because of the single central lobe confined to a region $\leq$ 100nm. In the following, the near-field distribution shown in Fig. 7(b) will be named a plasmonic virtual probe. Its electric field vector is oriented along the *y*-direction.

The presence of lateral lobes surrounding the virtual probe is undesirable for light nano-source applications. Sidelobe intensity is directly connected to DBR amplitude. As the modulation amplitude increases, the sidelobes are reduced, while the lateral extension of the SPP mode in the flat region remains unchanged. Unfortunately, a large modulation amplitude introduces strong perturbations of the SPP mode, leading to an increase in scattered light. We considered different modulation schemes in order to achieve an acceptable trade-off. An interesting result is reported in Fig. 8.

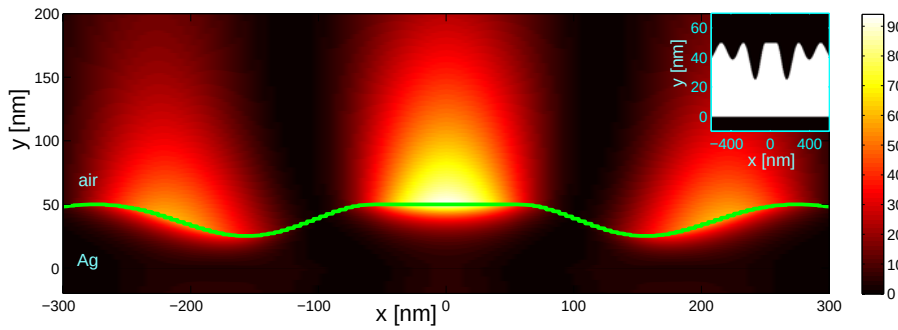

Fig. 8. Virtual probe excited in a cavity surrounded by a modified DBR (see inset for a detail). The squared amplitude of the magnetic field of the virtual probe is enhanced by a factor of 94 with respect to the incident plane wave. The effect of the overetched modulation is to reduce the intensity of the lateral lobes.

In this case, the first half-period of the DBR is etched with a much larger depth, which results in a more dramatic SPP damping and a consequent decrease of the sidelobe intensity. As expected, we found a larger diffraction efficiency ($T = 24\%$) for the transmitted light as compared to $T = 13.8\%$ calculated for the configuration of Fig. 7(b). The field enhancement factor at the metal-air interface is reduced to a value of $max\left\{|H_{SPP}(x,y)|^2\right\}/|H_0|^2 = 94$. In this configuration, the squared magnetic field distribution of the virtual probe close to the metal surface is described by a gaussian profile having $\sigma = 40$ nm. In conclusion, a better quality of the virtual probe can be obtained to the detriment of a smaller SPP coupling efficiency and a larger amount of transmitted light.

5. Scan of a small defect in a glass plate

One of the possible applications of the proposed plasmonic virtual probe is as light nano-source in a Scanning Near-field Optical Microscope system. As the excitation of SPP is highly sensitive to perturbations at the metal-air interface, the behavior of the plasmonic virtual tip when a sample is brought into close proximity constitutes an important topic to investigate. For this reason, the scan of a small object has been numerically simulated. In particular, we are interested in evaluating the contrast of the detected signals as the sample is scanned through the virtual probe. The considered sample consists of a flat glass plate having a small defect, whose profile is given by:

$$f(x) = \begin{cases} h \cdot exp\left[-\frac{(x+w-\Delta)^2}{s^2} \right] & x < -w \\ h & -w \le x \le w \\ h \cdot exp\left[-\frac{(x-w-\Delta)^2}{s^2} \right] & x > w \end{cases} \tag{3}$$

where $h = 50$ nm, $s = 10$ nm and $w = 20$ nm. The scanning variable Δ tracks the object lateral position with respect to the system of reference of the virtual probe. The sample must be placed close enough to the metallic structure to perturb the SPP: to this end we choose a distance of 100 nm from the cavity. In Fig. 9, the squared magnetic field in the region between the cavity and the sample is shown.

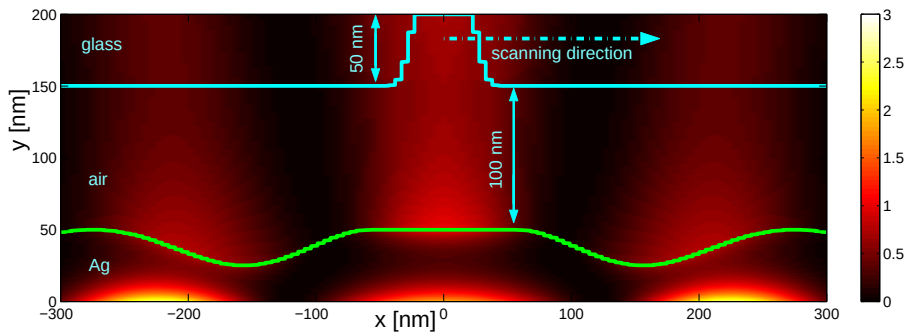

Fig. 9. A glass plate with a small defect is scanned by the virtual probe. The sample introduces a strong perturbation in the neighborhood of the metal surface that gives rise to a dramatic loss in the photon-plasmon coupling efficiency.

We remark that the energy contained in the SPP mode is strongly decreased due to the presence of the sample. The light is scattered into the transparent sample or reflected back into the glass with diffraction efficiencies $T = 24.25\%$ and $R = 72.25\%$ respectively and almost all of the energy hitting the silver film is re-radiated ($R + T = 96.5\%$). During the scan, the interaction of the sample with the virtual probe can be monitored by collecting the light scattered by the sample (T) or the light reflected by the silver film (R). As the defect moves in the positive x-direction, the $R(\Delta)$ and $T(\Delta)$ coefficients are calculated and plotted as functions of the defect position Δ (Fig. 10).

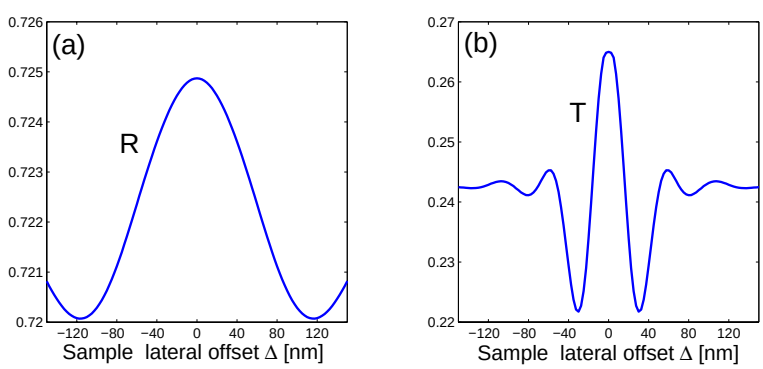

Fig. 10. (a) Reflection coefficient R and (b) transmission coefficient T calculated for different positions of the defect in the glass plate during the scan.

The curve in Fig. 10(a) represents the reflected light as the defect moves through the virtual probe. The overall modulation of the signal is very small ($\delta R \approx 0.5\%$) and its shape shows a central peak that is much broader than the extent of the defect. In particular, we observe that this curve is very similar to the squared field amplitude distribution of the SPP mode along the line $x = 150$ nm. We can argue that, as the lateral extension of the defect is smaller than the lateral dimensions of the virtual probe, the reflection coefficient profile reproduces the virtual probe squared field as probed by the defect itself. The profile shown in Fig. 10(b) represents the percentage of light that is transmitted into the glass plate. Here, the modulation is larger than in the previous plot ($\delta T \approx 4.2\%$) and its central peak much narrower. The profile shows the clear signature of the defect shape scanned through the virtual probe. Far away from the virtual probe, the modulation becomes negligible and the value of the transmission coefficient reaches the asymptotic value of $T = 24.25\%$. It is interesting to remark that the curves $R(\Delta)$ and $T(\Delta)$ are not directly correlated and the sum $R(\Delta) + T(\Delta)$ is not constant along the scan path. In order to explain this effect, absorption by the silver film must also be considered in addition to the radiative power (reflected and transmitted). Absorption is indeed proportional to the SPP coupling efficiency, that is highly sensitive to perturbations in close proximity of the metallic surface. In general we may say that, if perturbations are small, both reflected and transmitted power are small and viceversa, till a certain limit (depending on the kind of metallic structure) is reached. In the present case, as scatterer moves through the virtual probe, the plasmonic field is perturbed in a non-trivial way, leading the SPP coupling efficiency (and thus absorption) to vary significantly.

The simple situation considered here shows that objects having dimensions ≈ 50 nm can be detected with a relative contrast of $\delta T/T \approx 17.3\%$ by collecting the scattered light. On the other hand, the reflected light signal is weakly sensitive to objects smaller than the lateral extension of the virtual probe.

6. Summary and conclusion

Computational investigations on the application of a plasmonic virtual probe as a non-radiating nano-source in near-field microscopy have been performed.

We first demonstrated that such a virtual probe can be generated by a properly corrugated thin metallic film supporting SPP modes. The two-dimensional configurations considered in this paper are suitable for the generation of longitudinally polarized fields localized in a region < 100 nm wide. We also demonstrated that, within certain limitations, it is possible to enhance the characteristics of the virtual probe in terms of SPP excitation efficiency, field enhancement and sidelobes intensity.

Such a device is very sensitive to environmental conditions because of the plasmonic nature of the excited field. When resonance conditions are met, the strength of the excited plasmon field is strongly sensitive to small changes in the refraction index at the metallic/dielectric interface. This effect is widely exploited in plasmon-based sensors. We demonstrated that it can also be usefully exploited in a near-field scanning system. The scan of a small defect in a flat glass plate has been numerically performed. Two outputs have been considered: the light reflected from the silver-glass interface and the light scattered by the sample. In particular, we observe a strong modulation of the scattered light as the defect is scanned through the virtual probe. Such a signal modulation is essentially due to the plasmon sensitivity to refractive index perturbations in close proximity of the metallic surface. With the combined use of these two signals, it is possible, in principle, to detected small objects with dimensions of few tens of nanometers.

Acknowledgements

The authors greatly acknowledge W. Nakagawa for fruitful discussions on the computational aspects of the work.
This work has been supported by the E. U. grant no IST-2000-26479.